J Mater Sci: Mater Electron (2013) 24:1900–1904
DOI 10.1007/s10854-012-1032-y

A study of structural, ferroelectric, ferromagnetic, dielectric properties of $NiFe_2O_4$–$BaTiO_3$ multiferroic composites

Yanqing Liu · Yuhan Wu · Dan Li · Yongjun Zhang · Jing Zhang · Jinghai Yang

Received: 1 October 2012 / Accepted: 5 December 2012 / Published online: 14 December 2012

Abstract The mixed spinel-perovskite multiferroic composites of $xNiFe_2O_4$-$(1 - x)BaTiO_3$ ($x = 0.1, 0.2, 0.3, 0.4, 0.5, 0.6$) have been prepared by sol–gel method. The structure and morphology of the composites were examined by means of X-ray diffraction and transmission electron microscope. High-resolution transmission electron microscope image indicates a clear view of ferrite and ferroelectric phase. Moreover, we observed a fine interface between the two phases, where the coupling effect of ferrite and ferroelectric phase happened. The composites show excellent ferromagnetic and ferroelectric properties. The saturation magnetization (M_s) reaches to 24.139 emu/g for $x = 0.6$ at room temperature, the magnetization is about 2.37 emu/g for $x = 0.6$ when the temperature decreases to 90 k, and the polarization reaches to 3.75 $\mu C/cm^2$ for $x = 0.1$. Frequency dependent variations of dielectric constant and loss tangent for $xNiFe_2O_4$-$(1 - x)BaTiO_3$ were studied in detail.

1 Introduction

Multiferroic materials combined at least two ferroic orders have drawn more and more attentions for their potential applications such as waveguides, switching [1], modulation of amplitudes, transducers, and so on [2, 3]. The combination of both ferroelectric and ferromagnetic properties in a single material is expected to produce novel properties, such as magnetoelectric [4, 5], magnetooptic [6] and other new coupling properties, due to the coupling effects between the magnetization and electric polarization. According to the phenomenological theory, the magnetoelectric response of a single-phased material is limited by dielectric constant and magnetic permeability. Therefore, to obtain such multiferroic single-phased compound with large and robust ferromagnetic and ferroelectric ordering is still a challenge [7]. For this reason, multiferroic composites included ferromagnetic and ferroelectric materials are synthesized and studied widely. To achieve high performance, some important issues in the fabrication of composites should be taken into account. First, there must be no chemical reaction between ferroelectric and ferromagnetic phases during the sintering process. The chemical reaction can weaken the piezoelectric behaviour of ferroelectric phase and the magnetostrictive property of ferromagnetic phase. Second, the high magnetostriction coefficient of magnetic phase and large piezoelectric coefficient of piezoelectric phase are necessary. Then, to avoid the leakage path of accumulated charges, the resistivities of magnetostrictive phase must be high, and good dispersion of two phases is needed. Finally, for achieving good mechanical coupling, microstructure defects such as pores at the interface between the two phases must be avoided as possible.

Recently, some multiferroic composites have been successfully prepared. $BaTiO_3$ (BTO), PZT, $Pb(MgNb)O_3$ etc., are usually chosen as the piezoelectric phase, and ferrites are usually as the magnetic phase [8]. As a prototype, environmentally friendly ferroelectric material exhibited ferroelectricity at room temperature (RT) with steady chemical and mechanical properties, BTO has been

Y. Liu · Y. Wu · D. Li · Y. Zhang · J. Zhang · J. Yang (✉)
Institute of Condensed State Physics, Jilin Normal University, Siping 136000, People's Republic of China
e-mail: jhyang1@jlnu.edu.cn

Y. Liu · Y. Wu · D. Li · Y. Zhang · J. Zhang · J. Yang
Key Laboratory of Functional Materials Physics and Chemistry of the Ministry of Education, Jilin Normal University, Siping 136000, People's Republic of China

considered as one of the most widely used ferroelectrics [9] which had been studied in depth [10–12] and applied in the capacitors for several decades [13, 14]. Moreover, due to their large resistivities, ferrites can be used as magnetic materials. The spinel $NiFe_2O_4$ (NFO) ferrite is chosen for its large resistivity, low anisotropy, and high piezomagnetic coefficient. In addition, NFO ferrite shows the high initial permeability, which is one of the prerequisites for increasing the efficiency of ME conversion factors [15, 16]. However, few literatures were found to investigate NFO-BTO composites so systematically. In present work, we prepared xNFO-(1 − x)BTO composites by sol–gel method in order to expore various properties from different angles and lay a foundation for the future scientific research. XRD, TEM, and HRTEM are used to identify two phases, and the interface between ferrite and ferroelectric phases is studied. Moreover, the ferroelectric, magnetic and dielectric behaviors of the multiferroic composites are also investigated at length in the following.

2 Experimental details

Both of the NFO phase and the BTO phase were synthesized through sol–gel method. The NFO phase was prepared by mixing nickel nitrate hexahydrate [$Ni(NO_3)_2 \cdot 6H_2O$], iron nitrate nonahydrate [$Fe(NO_3)_3 \cdot 9H_2O$] and citric acid [$C_6H_8O_7 \cdot H_2O$] in the deionized-water with appropriate stoichiometric proportions. The mixture was stirred constantly for 2 h and dried for 24 h to obtain the precursor. Then, the precursor was annealed at 1,000 °C for 2 h to form spinel structure of NFO. For fabricating BTO phase, we choose bariumacetate [$Ba(CH_3Coo)_2$], titanium butoxide [$Ti(OC_4H_9)_4$], and acetylacetone [$CH_3COCH_2COCH_3$] as the initial materials. The glacial acetic acid was used as the solvent. First, barium acetate was added into glacial acetic acid. Then, the solution was stirred for 1 h. Second, acetylacetone and titanium butoxide were added into glacial acetic acid, and the solution was also stirred for 1 h. Third, the two transparent solutions were mixed together and a yellow transparent solution was formed after constant stirring. Finally, the solution was dried and sintered at 1,000 °C for 2 h to form the perovskite structure of BTO. The six kinds of mixed powder of xNFO-(1 − x)BTO with x = 0.1–0.6 in the molar ratio was ball-milled for 5 h. Then, the PVA binder solution was added to the powder. The powder was then pressed into six disks with the diameter of 10 mm and the thickness about 1 mm under the pressure of 26 Mpa, which were sintered at 1,200 °C for 3 h in air. At last, we obtained six dark samples. Moreover, for measuring the dielectric properties, silver electrodes were coated on the top and bottom surfaces of the samples.

The structure characterization was done using the X-ray diffractometer with CuKα radiation (40 kV, 200 mA). The morphology, interplanar distance and interface of the composites were investigated by transmission electron microscope (200 keV, JEM-2100HR). Ferroelectric tests were measured using a Precision PremierII (radiant technologies). Magnetic hysteresis loops of the composites were measured by a Lake Shore 7,407 vibrating sample magnetometer. Dielectric properties were measured using a LCR meter (HP4294A, Aglient).

3 Results and discussion

3.1 Structural characteristics

Figure 1 shows the X-ray diffraction (XRD) patterns of xNFO-(1 − x)BTO composites (x = 0.1, 0.2, 0.3, 0.4, 0.5, 0.6). All the peaks can be indexed according to perovskite BTO (card no. 05-0626) and spinel NFO (card no. 10-0325). No unidentified peaks are found from the XRD patterns, which indicates the absence of any chemical reaction between the two phases during the final sintering process. Moreover, the patterns indicate that even with x = 0.1, the diffraction peaks of NFO are observable. And, the intensity of NFO diffraction peaks increases with NFO content increasing while the intensity of the BTO diffraction peaks decreases. This means that the composites consist of BTO and NFO, it is reasonable because of the phase separation of pervoskite ABO_3 and spinel NFO [17, 18].

Figure 2 shows the TEM image of the composites. The image reveals that the average grain size is about 20 nm. The HRTEM image of the square region is shown in the inset of Fig. 2. Presence of both BTO and NFO phases

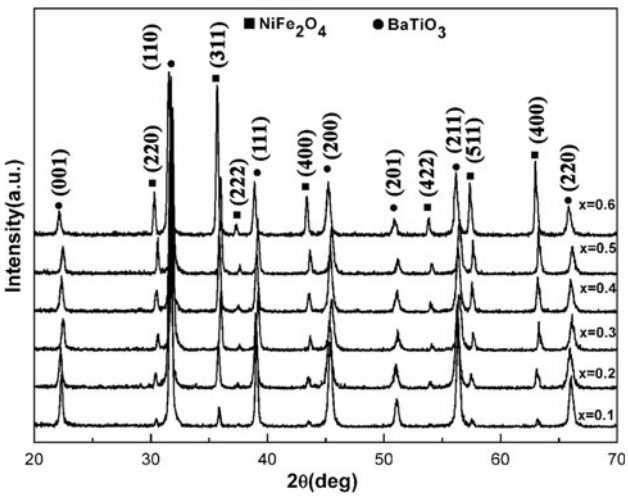

Fig. 1 XRD patterns of xNFO-(1 − x)BTO composites (x = 0.1, 0.2, 0.3, 0.4, 0.5, 0.6)

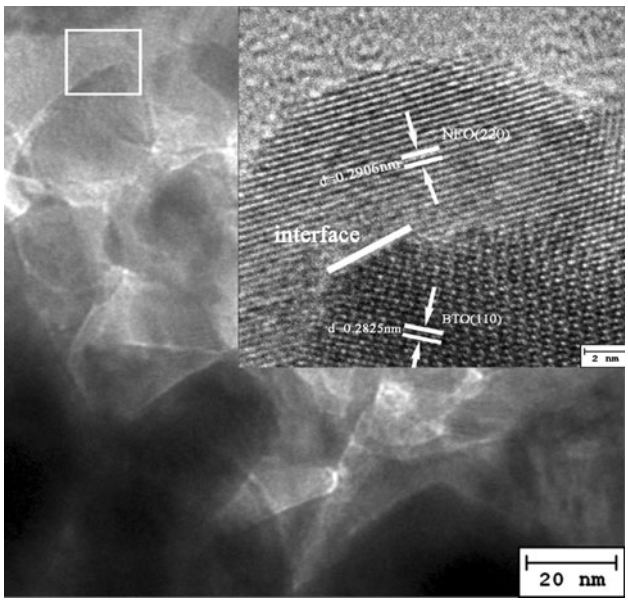

Fig. 2 TEM and HRTEM images of the composites

could be clearly observed, which is also confirmed by XRD. The calculated interplanar distance, 0.2825 nm, can be identified by the (110) plane of BTO phase (card no. 05-0626); the calculated interplanar distance, 0.2906 nm, can be identified by the (220) plane of NFO phase (card no. 10-0325). Moreover, the HRTEM image reveals a clear interface between NFO phase and BTO phase. Strain transition between the ferrite and ferroelectric phase could happen in the interface, which in turn realizes the coupling of ferroelectric and ferromagnetic ultimately. There are also some defects at the interface of the composites which may have negative influence on both magnetic and electric behaviors of multiferroic composites.

3.2 Ferroelectric properties

The ferroelectric properties of the NFO-BTO composites were examined by measuring the polarizations (P) against the electric field (E) up to 50 kV/cm, as shown in Fig. 3. From the ferroelectric hysteresis loops, excellent ferroelectric behavior was observed. The P_{max} reaches 3.75 μC/cm^2 of the composite with x = 0.1, which decreases to 0.69 μC/cm^2 with x = 0.6. Obviously, with the increasing of ferrite content, the measured P_{max} decreases. The low polarization of the composites is caused by the paraelectric effect of the NFO phase and the higher ferrite content [19]. When the NFO content reaches to x = 0.2, there is a sharp drop on P_{max} (2.08 μC/cm^2). After that, the P_{max} of composites decreases slowly with increasing NFO content. This suggests that there is a critical point for the NFO mole ratio around x = 0.1. The ability of polarization of the BTO phase is destroyed once the NFO mole ratio is beyond this

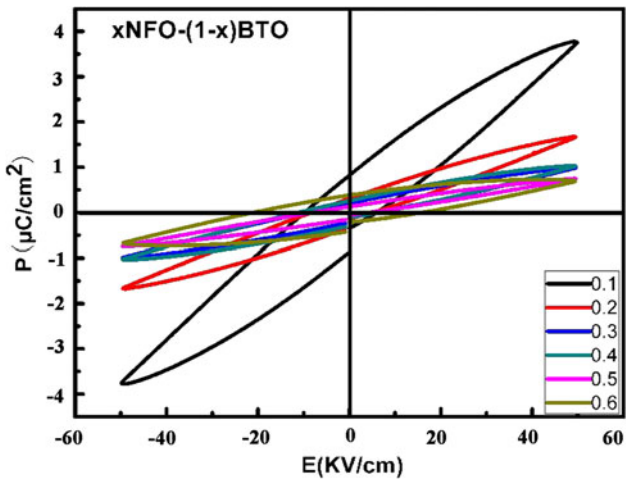

Fig. 3 The polarizations (P) against the electric field (E) of xNFO-(1 − x)BTO composites (x = 0.1, 0.2, 0.3, 0.4, 0.5, 0.6)

critical point. But there exists little tendency of leakage in the composites also.

3.3 Ferromagnetic properties

Magnetization-magnetic filed (M-H) loops of the xNFO-(1 − x)BTO (x = 0.1, 0.2, 0.3, 0.4, 0.5, 0.6) composites were measured at RT, as shown in Fig. 4. All the samples show saturated magnetization loops because of the presence of the ordered magnetic structure in the composites. The saturation magnetization (M_s) increases with the increasing of ferrite content, which increases from 3.506 emu/g for x = 0.1–24.139 emu/g for x = 0.6. The enhancement is because that the magnetic behaviour of nickel ferrite is related to cation distribution and Neel theory of ferrimagnetisms [20]. In the two phase system, the individual grains of the ferrite give contribution to the magnetization.

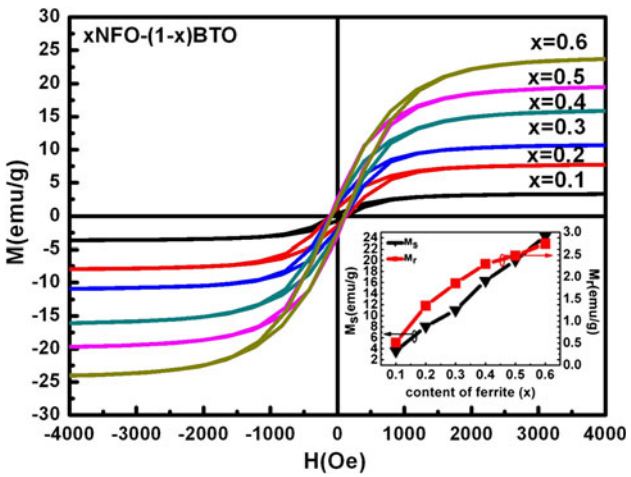

Fig. 4 Magnetization-magnetic filed (M-H) loops of xNFO-(1 − x) BTO composites (x = 0.1, 0.2, 0.3, 0.4, 0.5, 0.6)

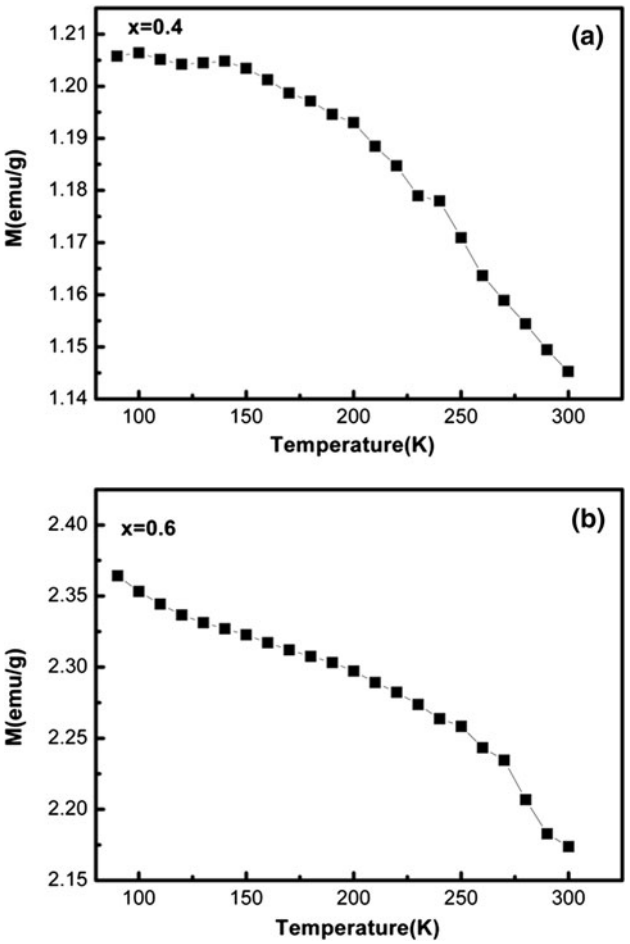

Fig. 5 Temperature dependent magnetization of xNFO-(1 − x)BTO composites with x = 0.4 and 0.6

However, the BTO grains next to the magnetic grains break the connection of magnetic grains, as seen in the inset of Fig. 2. Therefore, ferroelectric BTO grains act as pores and break the magnetic circuits. The results of our experiment are similar with what the literature reported before [21, 22].

The dependence of M_s and remnant magnetization (M_r) on the ferrite content can be observed more clearly in the inset of Fig. 4.

Temperature dependent magnetization of xNFO-(1 − x) BTO with x = 0.4 and 0.6 are shown in Fig. 5a, b. It can be seen that the magnetization increases as temperature decreases from RT to 90 K, which is in accordance with the temperature dependent magnetization of ferromagnetic [23]. Apparently, the magnetization of the composite with x = 0.6 is larger than that of x = 0.4. The magnetization of the composite with x = 0.4 trends to be saturated, while the magnetization with x = 0.6 trends to increase after the temperature decreases to 150 K. This is due to the increasing mole ratio of ferrite phase, which enhances the magnetization of composites, and the decreasing mole ratio of ferroelectric phase, which prevents the interaction between the magnetic particles more weakly.

3.4 Dielectric properties

The effects of frequency (range from 50 Hz to 1 MHz) on dielectric constant (ε_r) and dielectric loss (tanδ) of the composites are shown in Fig. 6. Figure 6a shows the frequency dependent ε_r of the composites. The ε_r of the composites decreases quickly with increasing frequency and reaches a constant value at higher frequency. The ε_r shows dispersion at lower frequency, which can be explained by Maxwell-Wanger interface polarization, which is in good agreement with Koop's theory [24–26]. The difference of the dielectric values in lower frequency is due to the inhomogeneity of two phase system. For the different permittivities and conductivities of ferrite phase and ferroelectric phase, when an electrical field is applied to the composites, the space charge carriers provided by NFO accumulate in the interface of two phases, which need finite time to make their axes parallel to the alternating electric filed [27]. At higher frequency range, the ε_r become independent of frequency,

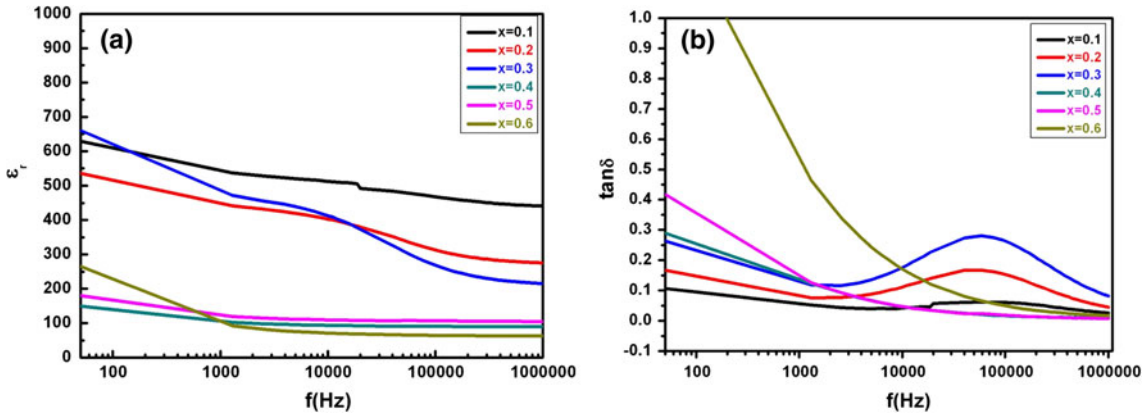

Fig. 6 The effects of frequency on dielectric constant (ε_r) and dielectric loss (tanδ) of xNFO-(1 − x)BTO composites (x = 0.1, 0.2, 0.3, 0.4, 0.5, 0.6)

this is due to the electric dipoles can not keep pace with the frequency of applied electric filed and only electronic polarization contributes to the ε_r at higher frequencies [28]. Figure 6b shows the frequency dependent tanδ of the composites. It reveals that the composites show abnormal tanδ as the ferrite content increases. According to Rezluscu [29], the abnormal behaviour of some ferrites is due to the collective behaviours of two types of charge carriers, i.e., *p* and n to the polarization.

4 Conclusion

In summary, through the sol–gel method and directly mixed way, we obtained the xNFO-(1 − x)BTO multiferroic composites. The structure, morphology, magnetic, ferroelectric and dielectric properties of xNFO-(1 − x) BTO composites have been studied. The coexistence of both spinel NFO and pervoskite BTO phase is confirmed by XRD and HRTEM. Observations of ferromagnetic and ferroelectric hysteresis loops indicate that excellent ferromagnetic and ferroelectric properties exist simultaneously at room temperature in the composites. The dielectric constant shows dispersion at lower frequency and independence of frequency at higher frequency. The composites show abnormal dielectric loss as the ferrite content increases.

Acknowledgments This work is supported by the National Natural Science Foundation of China (Grant Nos. 61178074), the National Youth Program Foundation of China (Grant Nos. 10904050), the Program for the development of Science and Technology of Jilin province (Item No. 201115218), the Natural Science Foundation of Jiangsu Province of China (BK2010348).

References

1. Y. Chen, T. Fitchorov, C. Vittoria, V.G. Harris, Appl. Phys. Lett. **97**, 052502 (2010)
2. C.W. Nan, N. Cai, L. Liu, J. Zhai, Y. Ye, Y. Lin, J. Appl. Phys. **94**, 5930 (2003)
3. K. Zhao, K. Chen, Y.R. Dai, J.G. Wan, J.S. Zhu, J. Appl. Phys. Lett. **87**, 162901 (2005)
4. S.V. Suryanarayana, Bull. Mater. Sci. **17**, 1259 (1994)
5. S. Lopatin, I. Lopatina, I. Lisnevskaya, Ferroelectrics **162**, 63 (1994)
6. T. Kanai, S.I. Ihkoshi, A. Nakajima, T. Watanabe, K. Hashimoto, Adv. Mater. **13**, 487 (2001)
7. J. Yu, J.H. Chu, Chin. Sci. Bull. **53**, 2097 (2008)
8. C.W. Nan, M.I. Bichurin, S.X. Dong, D. Viehland, G. Srinivasan, J. Appl. Phys. **103**, 031101 (2008)
9. H.X. Liu, B.B. Cao, C. O'Connor, J. Appl. Phys. **109**, 07 (2011)
10. M.B. Park, S.J. Hwang, N.H. Cho, Mater. Sci. Eng., B **99**, 155 (2003)
11. J.M. Oh, N.H. Kim, S.C. Choi, S.M. Nam, Mater. Sci. Eng., B **161**, 80 (2009)
12. T. Hiramatsu, T. Tamura, N. Wada, H. Tamura, Y. Sakabe, Mater. Sci. Eng., B **120**, 55 (2005)
13. L. Zhang, J.W. Zhai, W.F. Mo, X. Yao, Solid State Sci. **12**, 509 (2010)
14. X.W. Qi, J. Zhou, Z.X. Yue, Z.L. Gui, L.T. Li, S. Buddhudu, Adv. Funct. Mater. **14**, 920 (2004)
15. G. Srinivasan, E.T. Rgsmussen, H. Hayes, Phys. Rev. B. **67**, 14418 (2003)
16. A.S. Fawzi, A.D. Sheikh, V.L. Mathe, Phys. B **405**, 340 (2010)
17. S.T. Zhang, M.H. Lu, D. Wu, Y.F. Chen, N.B. Ming, Appl. Phys. Lett. **87**, 262907 (2005)
18. Y.K. Jun, W.T. Moon, C.M. Chang, H.S. Kim, H.S. Ryu, J.W. Kim, K.H. Kim, H.S. Hong, Solid State Commun. **135**, 133 (2005)
19. J.G. Wan, H. Zhang, X.W. Wang, D.Y. Pan, J.M. Liu, G.H. Wang, J. Appl. Phys. **89**, 122914 (2006)
20. V.G. Harris, IEEE Trans. Magn. **48**, 1075 (2012)
21. T. Kanai, S.I. Ohkoshi, A. Nakajima, T. Watanabe, K. Hashimoto, Adv. Mater. **13**, 487 (2001)
22. H.F. Zhang, P.Y. Du, Solid State Commun. **149**, 101 (2009)
23. S.T. Zhang, L.Y. Ding, M.H. Lu, Z.L. Luo, Y.F. Chen, Solid State Commun. **148**, 420 (2008)
24. J.C. Maxwell, *Electricity and Magnetism* (Oxford University Press, London, 1973)
25. K.W. Wagner, Ann. Phys. **40**, 818 (1993)
26. C.G. Koops, Phys. Rev. **83**, 121 (1951)
27. Y.J. Li, X.M. Chen, Y.Q. Lin, Y.H. Tang, J. Eur. Ceram. Soc. **26**, 2839 (2006)
28. S.A. Lokarea, R.S. Devana, B.K. Chougule, J. Alloys Compd. **455**, 471 (2008)
29. N. Rezluscu, E. Rezluscu, Phys. State Solid (a). **23**, 575 (1974)